Influence of the interaction volume on the kinetic energy resolution of a velocity map imaging spectrometer*

Peng Zhang(张鹏)[1], Zheng-Peng Feng(冯正鹏)[1], Si-Qiang Luo(罗四强)[1], and Zhe Wang(王哲)[2†]

[1] *Huazhong University of Science and Technology, Wuhan* 430074, *China*
[2] *Wuhan Institute of Technology, Wuhan* 430073, *China*

(Received 21 September 2015; revised manuscript received 11 November 2015; published online 10 February 2016)

We investigate the influence of the interaction volume on the energy resolution of a velocity map imaging spectrometer. The simulation results show that the axial interaction size has a significant influence on the resolution. This influence is increased for a higher kinetic energy. We further show that the radial interaction size has a minor influence on the energy resolution for the electron or ion with medium energy, but it is crucial for the resolution of the electron or ion with low kinetic energy. By tracing the flight trajectories we show how the electron or ion energy resolution is influenced by the interaction size.

Keywords: velocity map imaging, interaction size, resolution

PACS: 32.80.–t, 32.80.Fb, 33.60.+q, 07.81.+a **DOI:** 10.1088/1674-1056/25/3/033202

1. Introduction

Atoms and molecules exposed in a strong laser field[1] can be ionized, triggering many interesting strong-field phenomena, such as high-order harmonic generation[2,3] and dissociation[4–6] or ionization.[7–9] The kinetic energy (KE) distribution of the reaction products from the ionization or the dissociation is vital to investigate the molecular dynamics.[10–12] Several methods have been used to measure the KE distribution, e.g., time of flight (TOF) spectrometry[13–15] and ion/electron imaging spectrometry.[16–18] The ion/electron imaging technique is powerful for measuring the angular and KE distribution of ions/electrons at the same time. In a typical imaging experiment, the ions/electrons are produced by focusing the laser beam to the target gas. Then the particles are projected to a position-sensitive detector by applying the electrodes. With some reconstruction algorithms,[19–21] one can retrieve the three-dimensional velocity distribution from the two-dimensional projection. Due to the volume of the ionization area, the image is blurred and the resolution of the momentum significantly decreases. In 1997, Eppink and Parker introduced a technique called velocity map imaging (VMI).[22] Figure 1 shows a schematic of the VMI spectrometer. The field produced by the three electrode plates (repeller, extractor, and ground) acts as an electrostatic lens. The electrostatic lens focus the particles from different initial positions onto a ring in the detector plane when their initial KE is the same. Using this electrostatic lens method, the resolving capability of the imaging spectrometer is improved drastically.

The energy resolution is an important factor to appraise the performance of a VMI spectrometer. High resolution is very helpful to investigate the underlying dynamics of many physical phenomena. For instance, the resonant ionization shows some peaks which are very close to each other in the photoelectron KE spectra.[23–26] Moreover, Stark splitting[27–29] induces some fine structures in the KE spectra of photoelectrons. To distinguish such subtle structures, many new designs are proposed to improve the resolution of VMI spectrometers in recent years.[30–33]

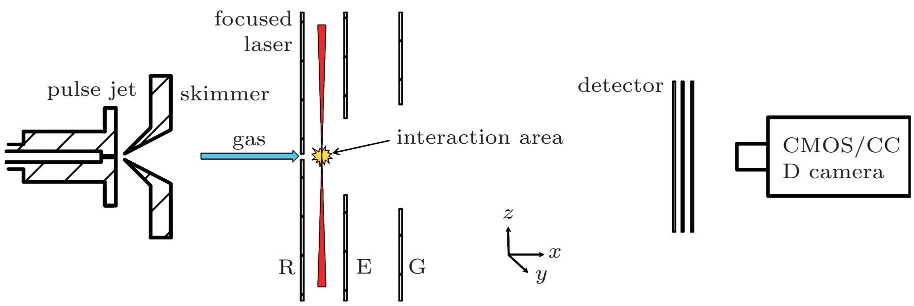

Fig. 1. (color online) Schematic of velocity map imaging spectrometer. R denotes repeller, E denotes extractor, and G denotes ground.

*Project supported by the National Natural Science Foundation of China (Grant Nos. 11234004 and 61275126).
†Corresponding author. E-mail: 972153190@qq.com

In a VMI spectrometer, the interaction size is one of the main factors which decreases the resolution. However, to our knowledge, no efforts have been dedicated to specifically investigate the influence of the interaction volume. In this article, we show how the interaction size affects the resolution in detail. The paper is organized as follows: in the next section, we show how the interaction size affects the resolution along radial direction and axial direction, respectively. In Section 3, we discuss the mechanisms of the influence along the two directions respectively. We conclude our work in Section 4.

2. Simulation results

In VMI experiments, the gas firstly passed through a gas jet and then was constrained by a skimmer which has an orifice in the center. The schematic of the skimmer is shown in Fig. 1. After passing through the skimmer, the gases spread and go through the hole of the repeller electrode before interacting with the laser beam. The hole diameter of the Repeller plate is generally a few millimeters, which is very large compared to the skimmer. Therefore, the gas beam size is mainly constrained by the skimmer orifice and it determines the interaction size along the radial direction of the flight tube (y–z plane in Fig. 1). Along the axial direction of the flight tube (x direction in Fig. 1), the interaction size is mainly determined by the laser beam diameter within the Rayleigh length. The laser beam diameter is small for tight focusing and it is large for loose focusing.

To investigate the influence of the size of interaction region to the resolution, we simulate the velocity map imaging experiments using the SIMION. The setups of the VMI spectrometer are schematically shown in Fig. 1. We use a cylinder to simulate the interaction region of laser and gas beams. The electrons are initially distributed in the cylindric region uniformly. The axis of the cylinder is along the x axis in Fig. 1. To investigate the influence to the resolution of different interaction size, we adopt three cylindric interaction regions of different sizes shown in Fig. 2. The length of cylinder A is 0.2 mm and the diameter is also 0.2 mm. Interaction region A corresponds to the situation that both the orifice diameter and the laser beam diameter are small. To investigate the influence of the interaction size along the axial direction (x in Fig. 1), we consider cylindric region B. The length of B is fifth of that of A, and the diameter is identical with A. Interaction region B corresponds to the situation that the orifice diameter of the skimmer is small but the laser beam diameter is large due to loose focusing. To investigate the influence of the interaction size along radial direction (y–z plane in Fig. 1), we consider cylindric region C. The length of C is identical with A and the diameter is fifth of that of A. The interaction region C corresponds to the situation that the orifice diameter of the skimmer is large, while the laser beam diameter is quite small due to tight focusing.

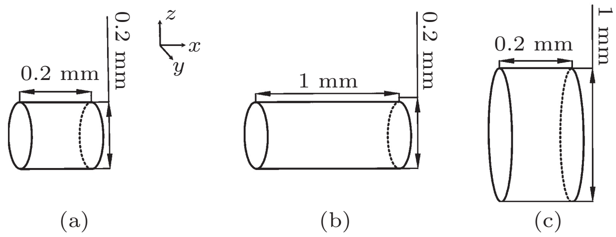

Fig. 2. Sizes of interaction region (a) A, (b) B, and (c) C in our simulation.

To achieve a good signal to noise ratio, we have simulated 1×10^6 electron trajectories in the interaction volume. One thing that should be noted is that the number of the particles generated in one laser shot is no more than 1000 to avoid space charge effect or other strong field effects in a typical VMI experiment. Then, to achieve a better signal to noise ratio, a large number of electrons are recorded in experiment. Those electrons are ionized by many laser shots. In our simulation, 1×10^6 electrons are ionized by many laser shots. Because a few particles are ionized in one laser shot, we have neglected the space charge effect in the simulation.

The initial KE distribution of the electrons is from 5 eV to 95 eV with an interval of 5 eV. The velocity directions distribute in the y–z plane uniformly. The KE range is common in a typical above-threshold ionization (ATI) process.[34–36] The voltage on the repeller is –5000 V, the one on the extractor is –3800 V, and the one on the ground plate is grounded. With the electric field constructed by the three electrode plates, the electrons are projected and focused to the detector plane. Electrons with identical KE are focused to a ring on the detector plane. Figures 3(a)–3(c) show the images recorded on the detector plane in the simulations with interaction regions of A, B, and C, respectively. The rings are formed by the positions that the electrons hit on the detector. The positions are in the range from –25 mm to 25 mm along the z direction. Different rings in the images correspond to different KE. We figured out the resolution by

$$\Delta E/E = 2(\Delta r/r), \tag{1}$$

where Δr is the width of the rings in the image, and r is the radius of the rings. Figure 4 shows the resolutions with three different interaction regions. By comparing the resolution of A and B, one can find that the resolution is significantly reduced with increasing the axial interaction size. Moreover, the difference between the two curves tends to be larger with the increase of the KE. This indicates that the influence is larger for high KE release. However, by comparison between A and C we can find that the difference between A and C is minimum at 60 eV and increases as the increase or decrease of the KE. This indicates that the changes of the size along the radial direction mainly affects the resolution of low KE and high KE, and the influence is minimum at the medium KE.

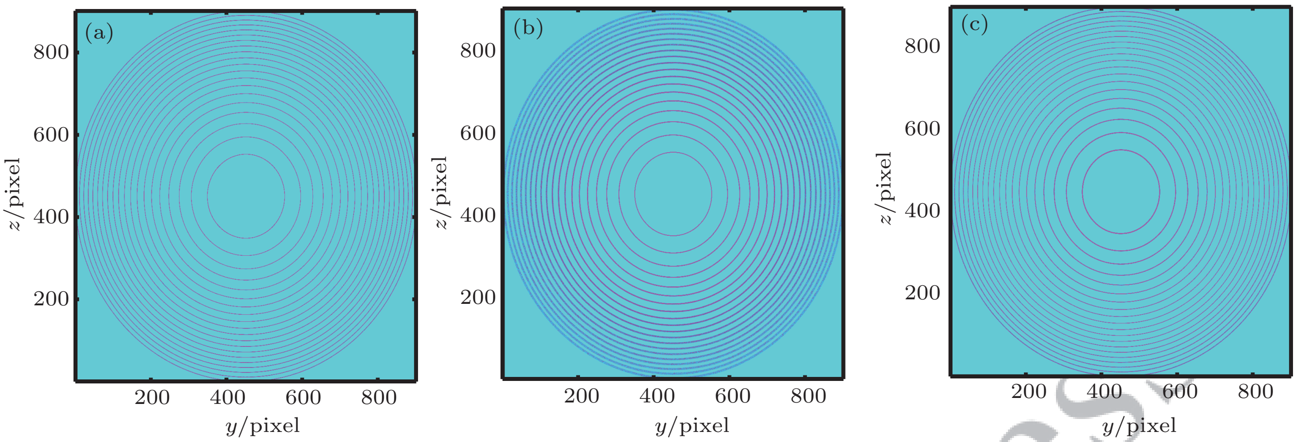

Fig. 1. (color online) The images recorded on the detector plane for VMI spectrometers (a) with interaction volume of A, (b) with interaction volume of B, and (c) with interaction volume of C in Fig. 2, respectively. The rings are formed by the positions that the electrons hit on the detector.

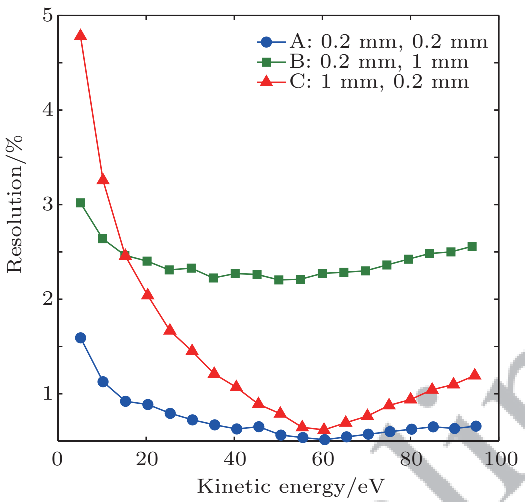

Fig. 4. (color online) Resolution curves obtained by Eq. (1) with different interaction sizes in simulation. A, B, and C correspond to the three interaction sizes in Fig. 2.

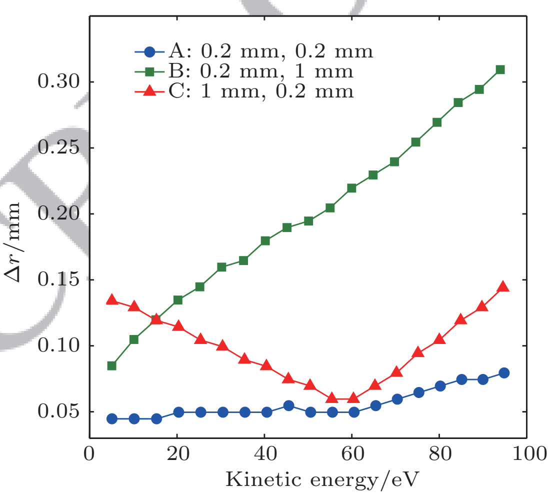

Fig. 5. (color online) The curves of Δr with different interaction sizes in simulation. A, B, and C correspond to the three different interaction sizes in Fig. 2.

To further investigate the influence of the interaction volume, we plot the curves of Δr (Eq. (1)) of Figs. 3(a)–3(c) in Fig. 5. By ignoring the denominator r in Eq. (1), the change of the resolution with respect to the KE can be clearly seen. By enlarging the size along the x direction from 0.2 mm to 1 mm (A to B), Δr of the high KE part (80–95 eV) increase by almost five times. While Δr of the low KE part (5–20 eV) only increase to twice of the value of A. This indicates that the influence of the axial interaction size is large for high KE. By enlarging the size along the y direction from 0.2 mm to 1 mm (A to C), Δr of the high KE part (80–95 eV) increase to three times of the value of A and Δr of the low KE part (5–20 eV) increase to nearly twice of the value of A. However, the value of Δr remains nearly unchanged at 60 eV. The results indicate that the radial interaction size mainly affects the particles with high or low KE, while the influence is minimum at the medium KE.

3. Discussion

3.1. Influence of the axial interaction size

In this section, we show how the interaction size affects the resolution with tracing the flight trajectories. Firstly, we discuss about the influence of the axial interaction size. The influence is induced by the time-of-flight difference of particles emitted from different axial positions. The maximum time-of-flight difference is directly determined by the axial interaction size. Larger time-of-flight difference will induce worse resolution. As a consequence, increase of the axial interaction size will reduce the resolution remarkably.

To find the difference between the influence for high KE release and that for low KE release, in Fig. 6, we simulate four electrons' flight trajectories. The electrons are from two different axial positions (e_3 and e_4 in the left panel). Two electrons releasing with 95 eV from 'e_3' and 'e_4', respectively, are focused to spot 'M' of the detector. Another two electrons releasing with 5 eV from 'e3' and 'e4', respectively, are focused to spot 'N' of the detector. From Fig. 6, one can find that the focused spot (M in the right panel) of electrons with 95 eV is larger than that with 5 eV (N in the left panel). In Fig. 6, the initial velocity of electrons is along the z axis to reflect typical experiments, as ionization occurs mainly along the laser polarization. Therefore, the time-of-flight of the electrons is independent of the initial KE. We assume the time-of-flight of the electrons from e_3 and e_4 as t_1 and t_2 respectively, and $\Delta t = t_2 - t_1$. We assume that v_1 is the initial velocity of the electrons with high KE, and v_2 is that with low KE. Then the spot size on the detector can be described as $v_1\Delta t$ for high KE, and $v_2\Delta t$ for low KE. Because $v_1 > v_2$, $v_1\Delta t > v_2\Delta t$. Therefore, the focus spot of electron with high KE is larger than that of electrons with low KE, which indicates that the axial interaction size affects the resolution of high KE more than that of low KE.

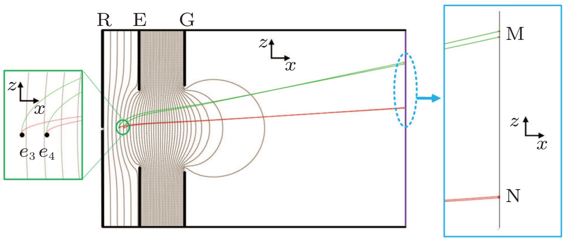

Fig. 6. (color online) The flight trajectories of two electrons with initial KE of 5 eV and two electrons with initial KE of 95 eV from two different axial positions. In the left enlarged view, e_3 and e_4 are the two different axial positions. In the right enlarged view, M is the focused spot of the two electrons with 95 eV, and N is the focused spot of that with 5 eV.

3.2. Influence of the radial interaction size

Then, we discuss the influence of the interaction size along radial direction. Figure 7 shows the flight trajectories of electrons from different radial positions and the axial interaction size is set to 0. The KE of the electrons ranges from 5 eV to 105 eV with an interval of 10 eV. The setups of the spectrometer and the voltages on the three electrode plates are identical with that in Section 2.

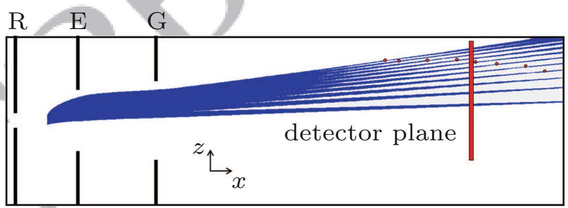

Fig. 7. (color online) Flight trajectories of electrons from different radial initial positions. The KE of the electrons ranges from 5 eV to 105 eV with an interval of 10 eV. The red spots are focuses of electrons with different KE. The red line is the detector plane.

With the introduction of electrostatic lens in VMI, the influence of the radial interaction size of the interaction volume is decreased. However, the electrostatic lens induce that ions/electrons with high KE which flying through the outside of the electrostatic lens focus earlier than that flying through the inside of the lens. In Fig. 7, the focuses of electrons are labeled with red spots. One can find that these focuses are located at different positions along the axial axis. In fact, the detector plane is generally placed near the focus point of electrons with medium KE. This is to balance the resolution of high KE and low KE release. Thus, on the detector plane, the spot's size is minimum for electrons with medium KE and large for electrons with low KE or high KE. With Eq. (1), one can easily find that the resolution will be best at the medium KE and worse as increase or decrease of the KE. The detector's position along the axial axis determine where the best resolution located in the KE spectra.

To explain the influence more clearly, in Fig. 8, we simulate six electrons' flight trajectories. The initial velocity of electrons is along the z axis. The six electrons are divided into three groups whose initial KE is 5 eV, 60 eV, and 95 eV, respectively. The two electrons of each group are emitted from two different radial positions (e_1 and e_2 on the left panel of Fig. 8). The electrons with 5 eV arrive the detector as a spot 'S' before the focal point. Thus, the spot size of S is larger than the beam size on the focal point. The electrons with 60 eV focus on the detector as a spot Q whose size is very small. The electrons with 95 eV focus before the detector and arrive the detector as a spot P, and the spot's size is also larger than that on the focal point. From the enlarged view shown in the right panel of Fig. 8, one can clearly find that the spot Q is obviously smaller than spot P and S. As a result, the resolution at 60 eV is better than that at 5 eV and 95 eV. This demonstrates that the radial interaction size's influence is depend on the detector's position along the axial axis. The radial interaction size mainly affects particles whose focal point is far away from the detector. In Section 2, the detector plane was located near the focus point of particles with 60 eV. As a consequence, there is a minimum influence to the resolution at 60 eV by the radial interaction size and the influence is quite large at low KE part and high KE part. Method was proposed to reduce the influence by radial interaction size.[37]

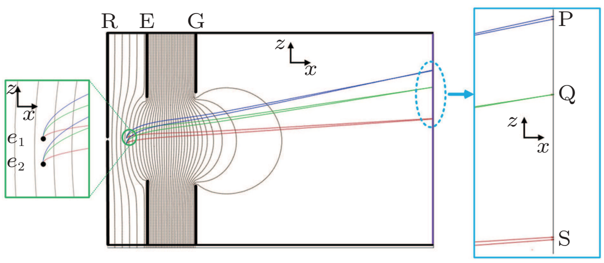

Fig. 8. (color online) The flight trajectories of three group of electrons with initial KE of 5 eV, 60 eV, and 95 eV, respectively. The two electrons of each group are emitted from two radial positions. The two initial positions e_1 and e_2 are shown in the left enlarged view. In the right enlarged view, P is the intersection spot of the electrons with 95 eV, Q is the intersection spot of electrons with 60 eV, and S is the intersection spot of electrons with 5 eV. In addition, the equipotential lines are shown.

4. Conclusion

With the simulation results, we found that increasing the axial interaction size would dramatically reduce the energy resolution of the VMI spectrometer. This influence becomes larger for a higher energy of the electrons or ions. It is because that the high-energy ions/electrons from different axial positions induce larger radial shift difference than the low-energy particles. Therefore, the focused rings of the ions/electrons with high KE is wider than that with low KE. For radial interaction size, the results show that the influence of the resolution is small for medium KE and large for lower KE or higher KE. The reason is that ions/electrons with high KE focus earlier than that with low KE and the focal points located in different positions along the axial axis. The detector plane is generally located near the focal point of the electrons with medium KE, hence the rings on the detector is narrow for medium KE and wide for high and low KE.

References

[1] Zhang N, Bao W X, Yang J H and Zhu X N 2013 *Chin. Phys. B* **22** 054209

[2] He L X, Lan P F, Zhai C Y, Li Y, Wang Z, Zhang Q B and Lu P X 2015 *Phys. Rev. A* **91** 023428

[3] Yang Y J, Chen J G, Chi F P, Zhu Q R, Zhang H X and Sun J Z 2007 *Chin. Phys. Lett.* **24** 1537

[4] Lan P F, Takahashi E J and Midorikawa K 2012 *Phys. Rev. A* **86** 013418

[5] Huang C, Lan P F, Zhou Y M, Zhang Q B, Liu K L and Lu P X 2014 *Phys. Rev. A* **90** 043420

[6] Jia Z M, Zeng Z N, Li R X, Xu Z Z and Deng Y P 2015 *Chin. Phys. B* **24** 013204

[7] Korneev P A, Popruzhenko S V, Goreslavski S P, Yan T M, Bauer D, Becker W, Kübel M, Kling M F, Rodel C, Wünsche M and Paulus G G 2012 *Phys. Rev. Lett.* **108** 223601

[8] Zhou Y M, Huang C, Liao Q and Lu P X 2012 *Phys. Rev. Lett.* **109** 053004

[9] Tong A H, Zhou Y M and Lu P X 2015 *Opt. Express* **23** 15774

[10] Posthumus J H 2004 *Rep. Prog. Phys.* **67** 623

[11] Li Y, Zhu X S, Lan P F, Zhang Q B, Qin M Y and Lu P X 2014 *Phys. Rev. A* **89** 045401

[12] Vredenborg A, Roeterdink W G and Janssen M H M 2008 *Rev. Sci. Instrum.* **79** 063108

[13] Wiley W C and McLaren I H 1955 *Rev. Sci. Instrum.* **26** 1150

[14] Guilhaus M, Selby D and Mlynski V 2000 *Mass Spectrom. Rev.* **19** 65

[15] Cheng J X, Ouyang X P, Zheng Y, Zhang A H and Ouyang M J 2008 *Chin. Phys. B* **17** 02881

[16] Heck A J R and Chandler D W 1995 *Annu. Rev. Phys. Chem.* **46** 335

[17] Thoman J W, Chandler D W, Parker D H and Janssen M H M 1988 *Laser Chem.* **9** 27

[18] Houston P L 1996 *J. Phys. Chem.* **100** 12757

[19] Smith L M, Keefer D R and Sudharsanan S I 1988 *J. Quant. Spectrosc. Radiat. Transfer* **39** 367

[20] Dribinski V 2002 *Rev. Sci. Instrum.* **73** 2634

[21] Vrakking M J J 2001 *Rev. Sci. Instrum.* **72** 4084

[22] Eppink A T J B and Parker D H 1997 *Rev. Sci. Instrum.* **68** 3477

[23] Wang P J and Fang Y 2008 *Chin. Phys. B* **17** 3668

[24] Wiehle R 2003 *Phys. Rev. A* **67** 063405

[25] Hertlein M P, Bucksbaum P H and Muller H G 1997 *J. Phys. B: At. Mol. Opt.* **30** L197

[26] Li M, Zhang P, Luo S Q, Zhou Y M, Zhang Q B, Lan P F and Lu P X 2015 *Phys. Rev. A* **92** 063404

[27] Georges A T and Lambropoulos P 1978 *Phys. Rev. A* **18** 587

[28] Liao Q, Zhou Y M, Huang C and Lu P X 2012 *New J. Phys.* **14** 013001

[29] Yu G H, Geng Y G, Li L, Zhou C, Duan C B, Chai R P and Yang Y M 2015 *Chin. Phys. B* **24** 103201

[30] Garcia G and Nahon L 2005 *Rev. Sci. Instrum.* **76** 053302

[31] Ghafur O, Siu W, Johnsson P, Kling M F, Drescher M and Vrakking M J J 2009 *Rev. Sci. Instrum.* **80** 033110

[32] Offerhaus H L, Nicole C, Lepine F, Bordas C, Rosca-Pruna F and Vrakking M J J 2001 *Rev. Sci. Instrum.* **72** 3245

[33] Skruszewicz S, Passig J, Przystawik A, Truongd N X, Kothera M, Tiggesbaumkera J and MeiwesBroera K H 2014 *Int. J. Mass. Spectrom.* **365** 338

[34] Kopold R, Becker W, Kleber M and Paulus G G 2002 *J. Phys. B: At. Mol. Opt. Phys.* **35** 217

[35] Deng Y K, Li M, Yu J Z, Liu Y X, Liu Y Q and Gong Q H 2014 *Chin. Phys. Lett.* **31** 064207

[36] Wang B B, Cheng T W, Li X F, Fu P M and Yu X G 2005 *Acta Phys. Sin.* **54** 3542 (in Chinese)

[37] Zhang P, Lan P F, Feng Z P, Zhang Q B and Lu P X 2014 *Meas. Sci. Technol.* **25** 105202